JOURNAL OF MATERIALS SCIENCE 29 (1994) 2281–2288

Measurement of Young's modulus and internal friction of an *in situ* Al–Al_3Ni functionally gradient material

Y. FUKUI
Department of Mechanical Engineering, Kagoshima University, 1-21-40, Korimoto, Kagoshima 890, Japan

K. TAKASHIMA
Department of Materials Science and Resource Engineering, Kumamoto University, 2-39-1, Kurokami, Kumamoto 860, Japan

C. B. PONTON
School of Metallurgy and Materials and IRM in Materials for High Performance Applications, The University of Birmingham, Edgbaston, Birmingham B15 2TT, UK

An *in situ* Al–Al_3Ni functionally gradient material (FGM) was produced by centrifugally casting an Al–20 mass% Ni alloy into a thick-walled tube. Four specimens, 90 mm long, with rectangular cross-sections (width × thickness) of 6 × 6, 6 × 5, 6 × 4 and 6 × 3 mm^2 were machined from the tube such that the thickness direction of the specimens was in the radial direction of the tube. The microstructure of the FGM tube consisted of granular morphology Al_3Ni as a second phase distributed within the aluminium matrix with an increasing volume fraction gradient from the inside to the outside of the tube. Thus, the thicker the specimen, the greater was the composition gradient and the thinner the specimen, the greater was the volume fraction of Al_3Ni. The dependence of the Young's modulus and internal friction on the composition gradient of the FGM was determined by a flexural forced-resonance technique from the resonant frequency and the resonance peak width, respectively, as a function of nominal specimen thickness. The Young's modulus of the Al_3Ni second phase was determined from a correlation plot of assumed Al_3Ni Young's modulus values against the calculated resonant frequency values corresponding to the associated FGM Young's modulus values. The latter were calculated using a rule of mixtures with a fixed matrix Young's modulus and a gradient volume fraction of Al_3Ni for each specimen thickness. By plotting the experimental FGM specimen resonant frequencies on this plot, the average Al_3Ni Young's modulus was found to be 140 GPa. The Young's modulus of the FGM was found to vary between 81.5 and 100.8 GPa across the 6 mm tube-wall thickness from the inner to outer surface, reflecting the 15.2 and 43.2 vol% Al_3Ni second phase, respectively. The measured internal friction increased with the volume fraction of Al_3Ni, and owing to the relatively large Al_3Ni particle size, was thereby dependent on the resultant increase in the second phase–matrix interface number density rather than the dislocation density.

1. Introduction

Intermetallic compounds are expected to exhibit unique combinations of mechanical, magnetic, electrical, and chemical properties, etc. However, the inherent brittleness of intermetallics prevents their commercial usage. Recently, the concept of a functionally gradient material (FGM) has been proposed for refractory materials [1]; a FGM is a kind of composite material that has a composition gradient in one direction, which is optimized for a specialized function (e.g. in the thickness direction). Thus, the idea need not be limited only to a refractory material, but applied also to materials for electrical and chemical applications. It is proposed that a new FGM be fabricated in order to benefit from the improved properties of intermetallics by minimizing the problems associated with their brittle nature.

One of the most well-known intermetallic compounds is Al_3Ni, and Al–Al_3Ni eutectic alloys have been used as a model material to examine the structure and properties of unidirectionally solidified reinforced material. The morphology of the Al_3Ni second phase changes from granular to fibrous depending on the solidification rate [2]. Based on these results, the feasibility of using Al_3Ni phase-distributed aluminium alloys as the basis of a FGM has been investigated.

0022–2461

Considering the Al–Ni phase diagram, molten alloys containing less than 30 mass % Ni can be used with the centrifugal casting method [3] to produce a thick-walled FGM tube. The intermetallic compound Al_3Ni is initially nucleated from the molten hypereutectic alloy containing 5.7 mass % Ni alloy. As the density of Al_3Ni is relatively high compared with the melt density, a graded radial distribution of the Al_3Ni phase within the tube cross-section is obtained. This graded distribution is caused by the differential centripetal forces experienced by the phases present, which depend on the phase density.

The potential uses of metal-intermetallic FGMs are numerous because of the wide range of property combinations. However, in terms of the possible structural or engineering applications, the dependence of the elastic properties on the composition gradient is a very important factor. Using the Young's modulus as an example, if the component materials' Young's modulus values are known, then a rule of mixtures can be applied to determine the Young's modulus of the FGM. The Young's modulus values reported for the Al_3Ni intermetallic compound differ markedly. For example, Hertzberg *et al.* [2] reported $E = 131$–152 GPa; Grabel and Cost [4] reported $E = 215$ GPa. The difference in the values appears to be related to the measurement technique employed and/or the phase crystallography. Thus, it is necessary to resolve this discrepancy in the Young's modulus of the Al_3Ni second phase. There are many methods for measuring the Young's modulus; measurement of the Young's modulus by a forced resonance technique is one of the most accurate methods. As far as the authors are aware this is the first reported use of flexural forced-resonance frequency measurements to determine the Young's modulus of a FGM.

In the present study, the effect of the composition gradient on the Young's modulus and internal friction of Al–Al_3Ni FGM specimens has been measured and analysed from the transverse free–free vibrations of rectangular beam specimens. The thickness of the rectangular beam specimens was varied to change the composition gradient of each specimen.

2. Experimental procedure

2.1. Materials

FGM was made by applying the centrifugal method [3] to an ingot of commercial purity Al–20 mass % Ni master alloy. The ingot was melted under an argon gas atmosphere at 890 °C and then cast into a 90 mm long thick-walled tube with an outer diameter of 90 mm and a wall thickness of 10 mm. The custom-made mould was rotated at a speed such that the molten metal experienced an acceleration equivalent to 23 times the gravitational acceleration. The crystal structure of Al_3Ni is $D0_{20}$ (*Pnma*) type and the unit cell size is $0.660 \times 0.735 \times 0.480$ nm [5]. The relative atomic masses of aluminium and nickel are 26.98 and 58.7, respectively; thus, the density of Al_3Ni is calculated to be 4000 kg m^{-3}, which is greater than the density of aluminium (2700 kg m^{-3}). The theoretical volume fraction of Al_3Ni in the master alloy is approximately 0.38. Owing to the density difference between Al_3Ni and aluminium–20 mass % Ni (molten) and the difference in the relative atomic masses of aluminium and nickel, each experiences a different centripetal force. Thus, a composition gradient is generated in the wall thickness direction. However, it is not known which factor is the dominant cause, i.e. the relative atomic mass difference or the phase-density difference. In any event, the volume fraction of Al_3Ni phase is expected to increase towards the outside of the tube.

2.2. Specimens

Initially, four ~ 90 mm long, square cross-section (6.1×6.1 mm^2) bars were machined from the cast tube such that the thickness direction of the bar corresponded to the radial direction of the tube as shown in Fig. 1. The bars were reduced in thickness by machining on an NC milling machine from the surface corresponding to the inside of the tube towards the outside surface of the tube. Thus, four rectangular bar specimens were obtained with nominal width × thickness dimensions of 6×6, 6×5, 6×4 and 6×3 mm^2, respectively. Hereafter, they are referred to as the 6, 5, 4 and 3 mm specimens, respectively. The accurate dimensions for each specimen are tabulated in Table I. The morphology of the Al_3Ni second phase and the composition gradient in the specimens were characterized by optical microscopy of metallographic samples prepared by standard metallographic polishing techniques.

2.3. Experimental apparatus for measuring Young's modulus

The apparatus used for the dynamic measurement of Young's modulus comprised conventional components arranged as shown schematically in Fig. 2. The sample is suspended in cotton-thread loops attached to the driver and detector, respectively. The loops are positioned 4 mm outside (or inside) the nodes corresponding to the fundamental flexural vibration

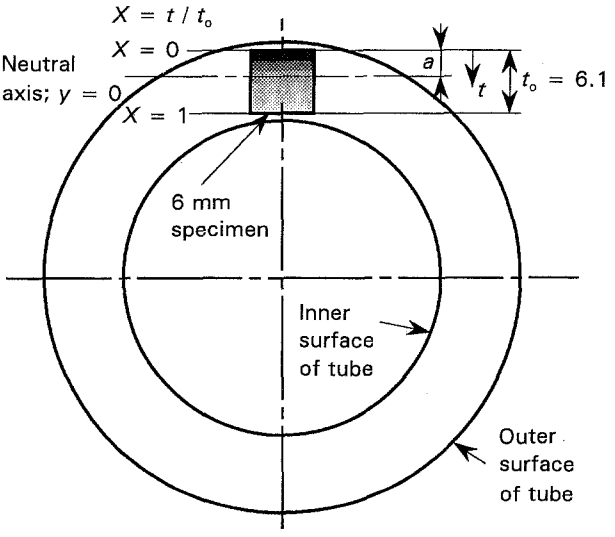

Figure 1 Schematic representation of FGM tube cross-section and showing the coordinate system used.

TABLE I Summary of measured specimen property values used for analysis

	Specimen			
	6 mm	5 mm	4 mm	3 mm
Thickness (mm)	6.10	5.02	4.05	3.01
Width (mm)	6.10	6.10	6.01	6.29
Length (mm)	89.90	90.14	90.05	90.03
Mass (g)	10.518	8.724	7.031	5.490
Average density ($kg\,m^{-3}$)	3144	3161	3208	3221
Resonant frequency (kHz)	4.111	3.409	2.774	2.077
Q^{-1} (10^{-3})	1.50	2.13	2.25	2.66

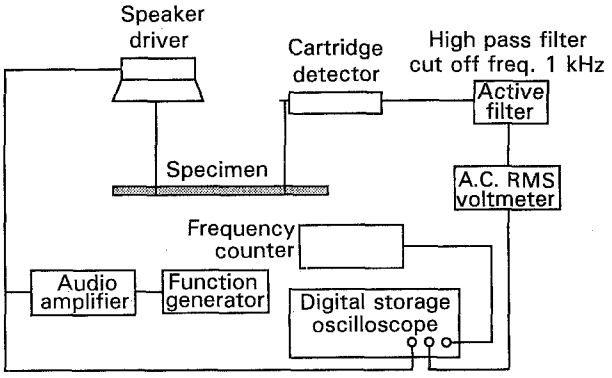

Figure 2 Block diagram of apparatus for determining Young's modulus and internal friction.

mode, i.e. at $0.224L$ and $0.776L$ where L is the specimen length. The constant output amplitude of the variable frequency oscillator is amplified and then sent to the driver. The frequency range 1–10 kHz is scanned until the driving frequency corresponding to one of the mechanical resonance frequencies of the specimen is determined.

The internal friction was determined by the resonance peak-width method in a simple manner [6]. The amplitude of the vibrational response is a maximum when the driving frequency and the natural resonant frequency of the specimen are equal, but decreases symmetrically about the resonant frequency to almost zero when the driving frequency is higher or lower than the resonant frequency. Thus, the internal friction at the resonant frequency, f_0, is given by

$$Q^{-1} = \Delta f/3^{1/2} f_0. \quad (1)$$

where $\Delta f = f_U - f_L$ and f_U and f_L are the driven frequencies above and below f_0, respectively, at which the vibrational amplitude is half that at f_0.

3. Dynamic determination of Young's modulus

3.1. Conventional equation for Young's modulus

The method of obtaining the Young's modulus of solid bodies from a knowledge of their mechanical resonance frequencies is well known and involves the solution of the differential equations for simple bending of a bar [7, 8]. The resonance frequency of a specimen, when the vibrational motion is transverse to the specimen's longitudinal axis and both ends of the specimens are unconstrained, is given by

$$(f_n)^2 = (k_n)^4 EIg/(2\pi)^4 \rho S L^4 T_n \quad (2)$$

where f_n is the resonant frequency of the nth vibrational mode, E the Young's modulus in the longitudinal axial direction, I the second moment of a finite area or moment of inertia, g the acceleration due to gravity, ρ the density, S the cross-sectional area, L the specimen length, T_n the correction factor, and k_n the solutions of

$$\cos(k_n)\cosh(k_n) = 1 \quad (3)$$

which are, namely, $k_0 = 0$, $k_1 = 4.7300$, $k_2 = 7.8532$, $k_3 = 10.9956$, $k_4 = 14.137$ and so on. The correction factor, T_n, for the fundamental mode of flexural vibration is given approximately [9] by

$$\begin{aligned} T_1 = {} & 1 + 6.585(1 + 0.0752\nu + 0.8109\nu^2)(t/L)^2 \\ & - 0.868(t/L)^4 - [8.340(1 + 0.2023\nu \\ & + 2.173\nu^2)(t/L)^4]/[1 + 6.338(1 + 0.14081\nu \\ & + 1.536\nu^2)(t/L)^2] \end{aligned} \quad (4)$$

where t is the specimen thickness and ν is Poisson's ratio. The fundamental flexural vibration mode was employed in the present study and $\nu = 1/3$ was assumed in the analysis because Poisson's ratio has little influence on the results.

3.2. Modification of theoretical resonant frequency equation

The microstructure of the material produced and used in this paper can be idealized as a dispersed particulate-reinforced metal matrix composite in which the distribution of particles is inhomogeneous, producing a composition gradient in the transverse thickness direction. In order to apply the above theoretical equation to such an inhomogeneous material system, the equation parameters which will be affected by the composition gradient must be identified. This has been done in the Appendix, which identifies E, I and ρ as the affected parameters. In the following analysis, it is assumed that the parameters E and ρ obey a simple rule of mixtures and are functions of the normalized position, X, in the thickness direction, where $X = 0$ and $X = 1$ denote the outer and inner surface of the FGM tube, respectively, as shown in Fig. 1.

Many equations describing the elastic moduli of composite materials have been reported; see, for example, [9]. However, a discussion of the relative merits of the various equations is not the aim of this paper. In the present work, the dependence of the FGM Young's modulus on composition is estimated by applying a simple rule of mixtures, as follows

$$E_{FGM} = E_m(1 - V_p) + E_p V_p \quad (5)$$

where V_p is the volume fraction of particles at position X, and E_m and E_p are the Young's moduli of the

matrix phase and the particulate phase, respectively. It is necessary to find out the position of the neutral axis or plane of bending which satisfies the following relationship for any transverse section

$$\begin{aligned} \int_S \sigma dS &= \int_S E_{FGM} \varepsilon dS \\ &= \int_S E_{FGM}(-y/R)dS \\ &= 0 \end{aligned} \quad (6)$$

where y is the distance from the neutral axis or neutral plane (at which $\sigma = 0$) in the transverse section as shown in Fig. 1 and R is the radius of curvature which is constant. The condition that the neutral axis passes through the centroid of the transverse section is

$$\int_S E_{FGM} y dS = 0 \quad (7)$$

Thus, we can calculate the EI value as

$$EI = \int_S E_{FGM} y^2 dS \quad (8)$$

We can also calculate the ρ_{FGM} in the transverse direction by again applying the rule of mixtures

$$\rho_{FGM} = \rho_m\{1 - V_p\} + \rho_p V_p \quad (9)$$

where ρ_m and ρ_p are the densities of the matrix and the particulate phase, respectively. Then, we can calculate the mean value of ρ as

$$\rho = \frac{1}{t}\int_0^t \rho_{FGM} dt \quad (10)$$

where t is the thickness of specimen. By substituting for EI from Equation 8 and for ρ from Equation 10 in Equation 2, the resonant frequency, f_n, of the FGM specimen can be calculated.

Clearly when both E_p and E_m are unknown, f_n cannot be calculated from Equation 2. However, if f_n is measured experimentally, then E can be determined provided the other parameters are known. Thus, if either E_p or E_m is known or measured, then E_m or E_p, respectively, can be calculated from Equation 5 assuming V_p is known. In the present work, E_m is known, and V_p, ρ_{FGM} and f_n are obtainable experimentally; thus, E_p can be calculated.

4. Results

4.1. Composition gradient

The thinnest specimen is expected to possess a smaller composition gradient and a higher volume fraction of Al_3Ni second phase. The distribution profiles of the Al_3Ni second phase in the aluminium matrix were obtained by quantitative optical microscopy. Optical micrographs of the second phase (Al_3Ni) morphology and distribution in specimens with $X = 0.39$ and $V_p = 0.38$ and with $X = 0.8$ and $V_p = 0.26$ are shown in Fig. 3a and b, respectively. The shape of the Al_3Ni second-phase particles varies from elongated to almost rectangular or square, while their sizes (i.e. diameters) are in the range of 30–150 μm. The specimens exhibit a composition gradient only in the thickness or transverse direction, i.e. radial direction of the tube as expected. The volume fractions of Al_3Ni phase as determined from each of the micrographs are plotted in Fig. 4 as a function of specific thickness; that is

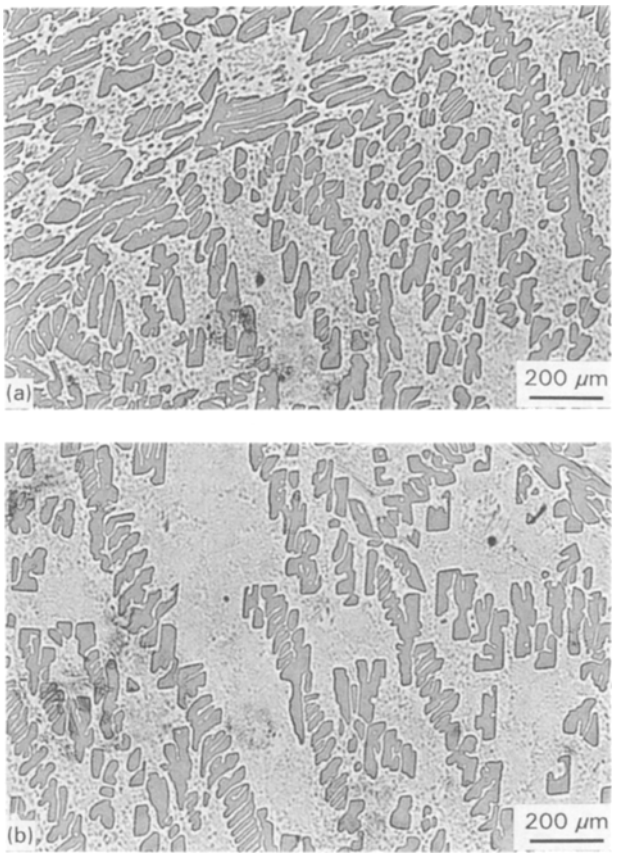

Figure 3 Optical micrographs showing the particle morphology and distribution of the Al_3Ni second phase in the aluminium matrix. The radial direction is from bottom to top. (a) $X = 0.39$ and 38 vol % Al_3Ni, (b) $X = 0.80$ and 26 vol % Al_3Ni.

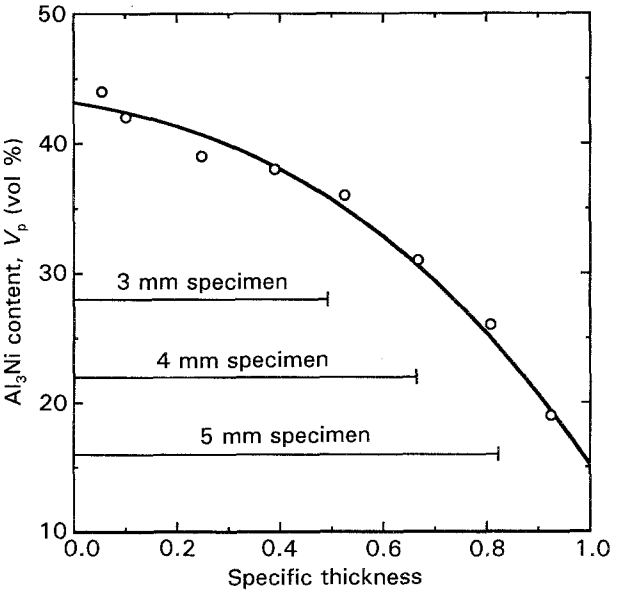

Figure 4 Volume per cent Al_3Ni, V_p%, as a function of specific thickness based on the 6 mm specimen. The bars indicate the effective specific thickness range of the other specimens. The plotted points are the measured V_p% values and solid line represents the best-fit curve through the experimental data.

the thickness of the specimen normalized with respect to the 6 mm specimen's thickness of $t_0 = 6.10$ mm where $X = 0$ and 1 correspond to the outer surface and inner surface of the tube, respectively, as shown in

Fig. 1. Therefore, the specific thickness for the 3, 4 and 5 mm nominal thickness specimens is $X = 0.493$, 0.664 and 0.823, respectively.

The Al_3Ni volume fraction distribution profile obtained is amenable to simple numerical analysis and is therefore described by

$$V_p\% = f(X) = -8.78(X + 0.489)^3 + 44.20 \quad (11)$$

which is the best-fit equation and is plotted in Fig. 4 as a solid line. The average volume per cent of Al_3Ni phase in the 6, 5, 4 and 3 mm specimens was 33.5%, 36.4%, 38.5% and 40.3%, respectively. The differences between the average densities based on Equation 10 employing $V_p\%$ values obtained from Equation 11 and those listed in Table I are in the range 0.10%–0.42%. Such small differences show that the composition gradient as described by Equation 11 is reasonably and sufficiently accurate for the analysis.

The Al_3Ni particle sizes were found to be dependent upon their location within the tube thickness. The Al_3Ni particle-size distributions in three sectioned regions of the 6 mm specimen, which coincided with the inner surface region, the interior and the outer surface region, respectively of the tube thickness, were determined. The number of particles were counted from 0 μm in size upwards in 10 μm wide bands, i.e. 0–10 μm, 10–20 μm, etc. The percentages in each band are shown in Fig. 5 by means of a histogram for each region. The peak of the distribution profile for the outer surface region is shifted towards small particle sizes. The mean particle sizes within the inner surface, interior and outer surface regions are 40, 50 and 70 μm, respectively.

4.2. Composition gradient dependence of Young's modulus

The flexural vibration resonant frequency decreased with decreasing specimen thickness. The measured resonant frequency for each specimen is given in Table I. Using Equations 5 and 2, a series of calculations were made to determine the resonant frequencies corresponding to FGM values dependent upon assumed E_m and E_p values in conjunction with the gradient V_p values for the 3, 4, 5 and 6 mm specimens. The assumed values for the Young's modulus of Al_3Ni were in the range $E_p = 80$–220 GPa, while the Young's modulus of the aluminium matrix was taken as $E_m = 71$ GPa. Thus, each assumed E_p value corresponds to a calculated resonant frequency, and for each specimen there is a set of such data. These data are plotted as Young's modulus of Al_3Ni against calculated FGM resonant frequency by the solid graph lines in Fig. 6. The greater the assumed E_p value the greater will be the calculated FGM resonant frequency. The Young's modulus of Al_3Ni can now be obtained directly from Fig. 6 if each specimen's experimental resonant frequency is plotted on the appropriate graph line.

The average Young's modulus of the Al_3Ni phase was found to be $E_p = 140$ GPa and the difference between the measured and calculated resonant frequencies for $E_p = 140$ GPa was less than 0.2%. Therefore, the Young's modulus of Al_3Ni is determined to be 140 GPa on the assumption of a rule of mixtures applying to a series of Al–Al_3Ni FGM specimens with different average volume fractions of Al_3Ni. This value compares well with the reported values of 131–152 GPa [2]. Using $E_p = 140$ GPa, the calculated Young's modulus variation within the 6 mm specimen as a function of specific thickness, and hence V_p, is shown in Fig. 7; the maximum and minimum values are 100.8 and 81.5 GPa, respectively. The corresponding Young's modulus variations for the 5, 4 and 3 mm specimens, with specific thickness ranges of $X = 0$–0.823, $X = 0$–0.664 and $X = 0$–0.493, respectively, are indicated by the horizontal lines in Fig. 7.

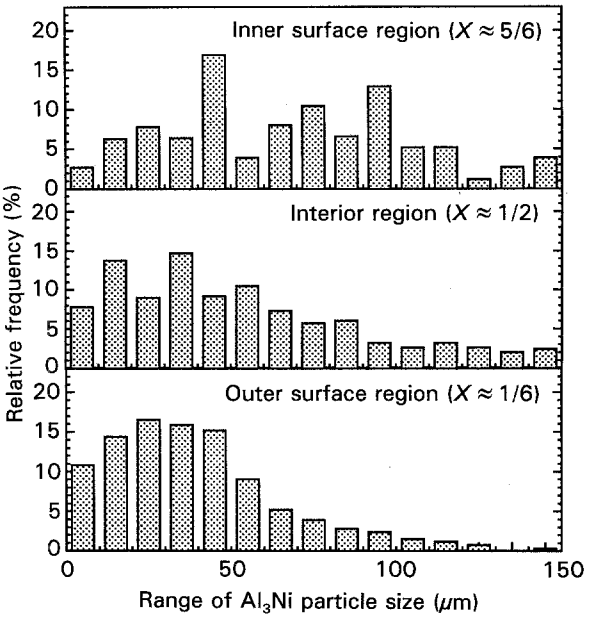

Figure 5 Histograms comparing the Al_3Ni particle-size distribution within three regions in the 6 mm specimen. The number of particles in each 10 μm band is divided by the total number of particles sized.

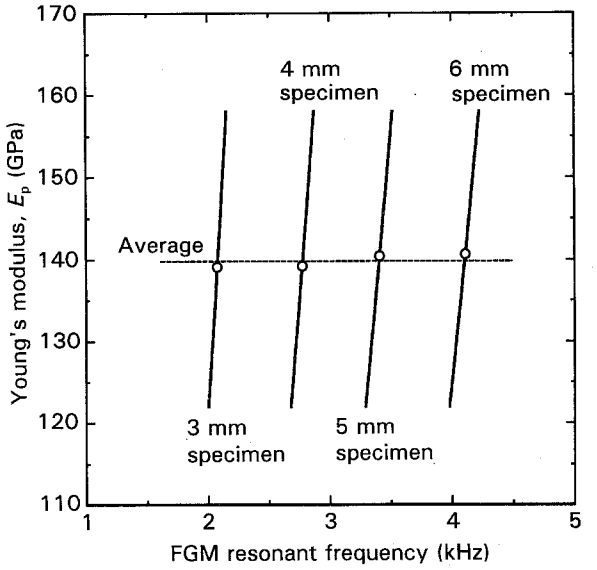

Figure 6 Relationship between the calculated E_{FGM} resonant frequency and the assumed Young's modulus of Al_3Ni, E_p. The plotted points are the experimental resonant frequency values obtained for each specimen.

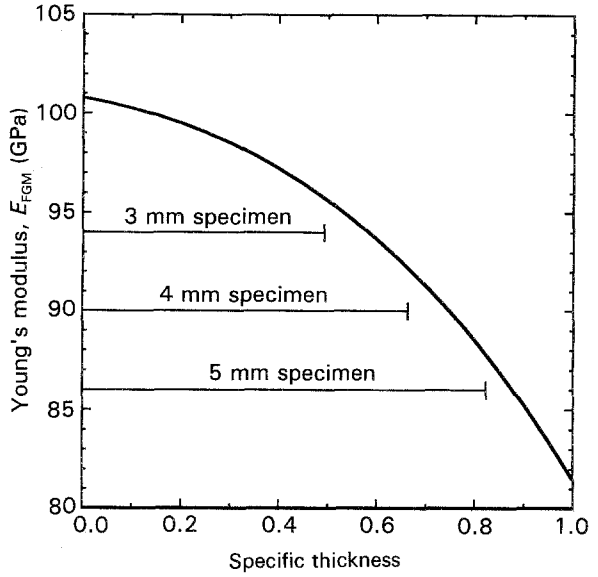

Figure 7 Calculated variation in Young's modulus as a function of specific thickness for the 6 mm thickness specimen. The bars indicate the specific thickness range of the other specimens.

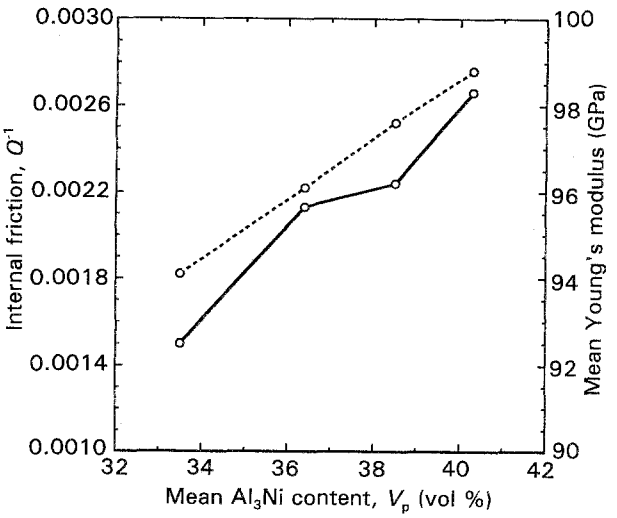

Figure 8 (——) Internal friction and (– – –) mean Young's modulus as functions of the mean volume per cent of Al_3Ni, V_p%.

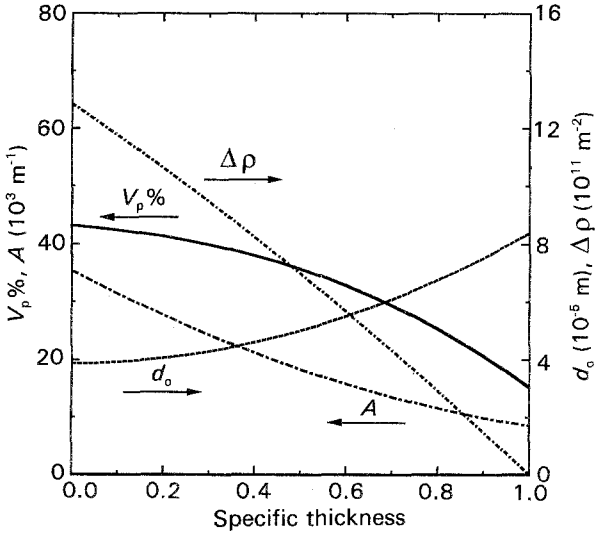

Figure 9 Volume per cent of Al_3Ni particles (V_p%), mean values of particles size, d_0, interface density, A, and increment of dislocation density, $\Delta\rho$, as a function of specific thickness.

4.3. Internal friction measurement

The relationship between the internal friction, Q^{-1}, and the mean volume fraction of Al_3Ni particles is shown in Fig. 8 and tabulated in Table I. The measured internal friction must be the average value for each FGM specimen because of the composition gradient within each specimen. The internal friction of the present FGM material increases with increasing mean volume fraction of Al_3Ni. The internal friction of a material is affected by microstructural features such as point defects, second phases in solids, dislocations and interfaces, all of which contribute to the energy dissipation occurring within the material when it is strained elastically. The number density of these features increases with increasing mean volume fraction of Al_3Ni in the FGM.

5. Discussion

The mean Young's moduli for the 6, 5, 4 and 3 mm specimens were calculated, using Equation 5, to be 94.1, 96.1, 97.6 and 98.8 GPa, respectively, as shown in Fig. 8. If the materials are assumed to be homogeneous, then direct calculation of E from Equation 2 gives values of 92.8, 95.5, 96.8 and 98.3 GPa for the 6, 5, 4 and 3 mm specimens, respectively. As the composition gradient within the specimen increases, so does the calculation error caused by assuming a homogeneous composition and using Equation 2 directly. Hence, a rule of mixtures should be used to calculate the average Young's modulus rather than the specimen resonant frequency–Young's modulus relationship when an FGM is under investigation.

In the present study, the effect of dislocation and second phase–matrix interface number density on the internal friction behaviour of the FGM has been considered. In the quantitative evaluation of the interface number density, it is assumed that the intermetallic's second phase is of spherical or cubic morphology, enabling easy calculation of the interfacial area per unit volume, i.e. the interface number density, ρ_I (m^{-1}). The dislocation density (m^{-2}) must be increased by thermal misfit strain according to Taya and Arsenault [10] or Kim *et al.* [11] who applied such an analysis to metal matrix composites. If a prismatic punching model [10] is assumed to be a mechanism for generating dislocations due to thermal strains in the present material, the dislocation density varies as $V_p/[(1 - V_p)d_0]$, where d_0 is the mean diameter of the particles. This relationship shows that the dislocation density increases with increasing second-phase volume fraction and particle size. The interface number density also depends on the second-phase volume fraction and particle size as $V_p d_0^2$.

The mean values of the particles' size, and hence the interface density and dislocation density are calculated on the basis of these second-phase particle size distributions shown in Fig. 3 and their volume fractions. These parameters are plotted as a function of

specific thickness in Fig. 9 and are represented by curves. As the volume fraction of Al_3Ni increases, the mean particle diameter is decreased and the interface density and dislocation density are increased. Likewise, the internal friction increases with increasing volume fraction of Al_3Ni. However, the real dislocation density, ρ, is given by $\rho = \rho_0 + \Delta\rho$ where ρ_0 is the dislocation density in the matrix alloy ($\sim 5 \times 10^{12}$ m^{-2}) [11]. In the present work, the value of $\Delta\rho$ is relatively small compared with ρ_0, unlike the case referred to by Taya and Arsenault [10] and by Kim *et al.* [11] and the effect of $\Delta\rho$ on the internal friction of the FGM may be ignored due to the relatively large second-phase particles observed. Thus, it may be concluded that the internal friction increases with increasing Al_3Ni volume fraction due mainly to the resultant increase in the interface density rather than the dislocation density.

6. Conclusions

In the present study, the effect of a composition gradient on the Young's modulus and internal friction of an Al–Al_3Ni functionally gradient material (FGM) has been determined by the measurement of flexural resonant frequencies using a forced-resonance technique on four rectangular bar specimens of differing thickness and hence composition. The results of the work are summarized below.

1. The average volume fraction of the granular Al_3Ni second phase in an Al–Al_3Ni FGM manufactured by a centrifugal casting method was found to be 33.5, 36.4, 38.5 and 40.3 vol % for the nominal 6, 5, 4 and 3 mm thickness specimens, respectively.
2. The Young's modulus of the Al_3Ni second phase was determined from the measured resonant frequencies as 140.6, 140.4, 139.2 and 139.1 GPa for the nominal 6, 5, 4 and 3 mm thickness specimens, respectively, by applying a rule of mixtures. The average Young's modulus of the Al_3Ni second phase is thus 140 GPa.
3. The Young's modulus variation within the 6 mm thick bar specimen ranged from a maximum of 100.8 GPa to a minimum of 81.5 GPa, corresponding to an Al_3Ni content of 43.2 and 15.2 vol %, respectively.
4. The internal friction of the FGM increases with increasing mean volume fraction of Al_3Ni and appears to depend mainly on the resultant increase in the interface density.

Acknowledgements

The work presented in this paper has been partly financed by the Iketani Science and Technology Foundation under the contract 041108BA in Japan. The contributions of Professor J. F. Knott FRS FEng and Dr P. Bowen, School of Metallurgy and Materials, University of Birmingham, are gratefully acknowledged.

Appendix. Basis of Equation 2

For the simple bending of a beam, the strain, ε, is given by

$$\varepsilon = -y/R \tag{A1}$$

where R is radius of curvature of the neutral axis of the beam and y is the distance from the neutral axis. Thus, stress, σ, is written as

$$\begin{aligned}\sigma &= E_{FGM}\varepsilon \\ &= -E_{FGM}\,y/R\end{aligned} \tag{A2}$$

Then, the applied bending moment, M, is

$$\begin{aligned}M &= -\int_S y\sigma \mathrm{d}S \\ &= (1/R)\int_S E_{FGM}\,y^2 \mathrm{d}S\end{aligned} \tag{A3}$$

where S is the cross-sectional area of the transverse section. In general, a radius of curvature, R, in an x–y coordinate system is given by

$$\begin{aligned}1/R &= (\mathrm{d}^2y/\mathrm{d}x^2)/[1 + (\mathrm{d}y/\mathrm{d}x)^2]^{3/2} \\ &\approx \mathrm{d}^2y/\mathrm{d}x^2\end{aligned} \tag{A4}$$

because $[1 + (\mathrm{d}y/\mathrm{d}x)^2]^{3/2} \approx 1$ since $(\mathrm{d}y/\mathrm{d}x)^2 \approx 0$.

Substituting Equation A4 into Equation A3, we get

$$M = (\mathrm{d}^2y/\mathrm{d}x^2)\int_S E_{FGM}\,y^2 \mathrm{d}S \tag{A5}$$

However, a shear force, F, is also acting during the bending of the specimen. This condition is written as

$$\partial F/\partial x = (\partial^2 y/\partial t^2)\,\rho S/g \tag{A6}$$

where t is time, ρ is the density and g is the acceleration due to gravity. Now

$$F = -\partial M/\partial x \tag{A7}$$

and so substituting Equation A5 for M in Equation A7 and differentiating results in

$$F = -\int_S E_{FGM}\,y^2 \mathrm{d}S\,(\mathrm{d}^3y/\mathrm{d}x^3) \tag{A8}$$

Now substituting Equation A8 for F in Equation A6 and differentiating gives

$$-\int_S E_{FGM}\,y^2 \mathrm{d}S\,(\mathrm{d}^4y/\mathrm{d}x^4) = (\mathrm{d}^2y/\mathrm{d}t^2)\rho S/g$$

By rearranging and multiplying through by $g/\rho S$, this equation can be rewritten as

$$(\mathrm{d}^2y/\mathrm{d}t^2) + (\mathrm{d}^4y/\mathrm{d}x^4)\{\int_S E_{FGM}\,y^2 \mathrm{d}S\}g/(\rho S) = 0 \tag{A9}$$

The solution of Equation A9 can be expressed in the form of Equation 2 for homogeneous materials. Noting that $I = \int_S y^2 \mathrm{d}S$ where I is the moment of inertia, it is clear that a gradient in the composition of the FGM across the transverse section (i.e. y direction) will affect E_{FGM}, I and ρ. The term $\{\int_S E_{FGM}\,y^2 \mathrm{d}S\}g/(\rho S)$ in Equation A9 is calculated considering a gradient in the composition through Equations 8 and 10, and then solved in the same manner as for homogeneous materials. Thus, the application of Equation 2 to an FGM has to take this into account, as discussed in Section 3.2.

References

1. M. KOIZUMI and Y. TADA, *Kinzoku* **58** (1988) 2 (in Japanese).
2. R. W. HERTZBERG, F. D. LEMKEY and J. A. FORD, *Trans. AIME* **233** (1965) 342.
3. Y. FUKUI, *JSME Int. J. Ser. III* **34** (1991) 2.
4. J. V. GRABEL and J. R. COST, *Metall. Trans.* **3** (1972) 1973.
5. F. D. LEMKEY, R. W. HERTZBERG and J. A. FORD, *Trans. AIME* **233** (1965) 334.
6. J. L. LYTTON, J. A. HREN, K. T. KAMBER and O. D. SHERBY, *Br. J. Appl. Phys.* **15** (1964) 1573.
7. G. PICKETT, *Proc. ASTM* **45** (1945) 846.
8. ASTM Designation: C623-71 "Standard Method of Test for Young's Modulus, Shear Modulus, and Glass-Ceramics by Resonance" (American Society for Testing and Materials, Philadelphia, PA, 1978).
9. T. W. CLYNE and P. J. WITHERS, "An Introduction to Metal Matrix Composites" (Cambridge University Press, Cambridge, 1993).
10. M. TAYA and R. J. ARSENAULT, "Metal Matrix Composites", (Pergamon Press, Oxford, 1989).
11. C. T. KIM, J. K. LEE and M. R. PLICHTA, *Metall. Trans.* **21A** (1990) 673.

Received 30 September
and accepted 1 November 1993